Novel Hepatitis B Virus Capsid Assembly Modulator Induces Potent Antiviral Responses *in Vitro* and in Humanized Mice

Franck Amblard[1#], Sebastien Boucle[1#], Leda Bassit[1], Bryan Cox[1], Ozkan Sari[1], Sijia Tao[1], Zhe Chen[1], Tugba Ozturk[1], Kiran Verma[1], Olivia Russell[1], Virgile Rat[2], Hugues de Rocquigny[2], Oriane Fiquet[3,4], Maud Boussand[3,4], James Di Santo[3,4], Helene Strick-Marchand[3,4], and Raymond F. Schinazi[1*]

[1] Center for AIDS Research, Laboratory of Biochemical Pharmacology, Department of Pediatrics, Emory University School of Medicine, 1760 Haygood Drive, Atlanta, GA 30322, USA;

[2] Morphogenèse et Antigénicité du VIH et des Virus des Hépatites, Inserm – U1259 MAVIVH, Hôpital Bretonneau, 10 boulevard Tonnellé – BP 3223 37032 Tours Cedex 1, France;

[3] Innate Immunity Unit, Institut Pasteur, 75724 Paris, France;

[4] Inserm U1223, 75724 Paris, France;

Running title: Efficacy of HBV Capsid Assembly Modulator

Dr. Raymond F. Schinazi, Center for AIDS Research, Laboratory of Biochemical Pharmacology, 1760 Haygood Drive, Atlanta, GA 30322, USA. Telephone: +1-404-727-1414. Email: rschina@emory.edu

[#]Contributed equally

Keywords: Capsid, hepatitis B virus, antiviral, cccDNA

Abstract

Hepatitis B virus (HBV) affects an estimated 250 million chronic carriers worldwide. Though several vaccines exist, they are ineffective for those already infected. HBV persists due to the formation of covalently-closed circular DNA (cccDNA) – the viral minichromosome – in the nucleus of hepatocytes. Current nucleoside analogs and interferon therapies rarely clear cccDNA, requiring lifelong treatment. Our group identified GLP-26, a novel glyoxamide derivative that alters HBV nucleocapsid assembly and prevents viral DNA replication. GLP-26 exhibited single-digit nanomolar anti-HBV activity and inhibition of HBeAg secretion, and reduced cccDNA amplification in addition to a promising pre-clinical profile. Strikingly, long term combination treatment with entecavir in a humanized mouse model induced decrease in viral loads and viral antigens that was sustained for up to 12 weeks after treatment cessation.

Introduction

Despite the availability of effective vaccines, epidemiologic data estimate that approximately 250 million people are chronically infected with hepatitis B virus (HBV) (more than the HIV and HCV carriers combined) and are at high risk for development of hepatitis, cirrhosis and hepatocellular carcinoma (1). Current anti-HBV treatment options include pegylated interferon alpha2a (pegIFN) and/or nucleoside analogs that require lifetime use to suppress the virus. Two key events in the HBV replication cycle involve first the generation of cccDNA transcriptional template, either from input viral DNA or newly replicated capsid-associated DNA, and second, reverse transcription of the viral pre-genomic (pg) RNA to form HBV DNA genomes that are encapsidated into de novo viral particles (2). HBV persists in long-lived hepatocytes due to the establishment and maintenance of cccDNA in the nucleus of host cells (3) where it is not targeted by current therapies and serves as a viral reservoir (4). Since hepatocytes have a long half-life, elimination of cccDNA by hepatocyte

turnover can be considered as a means of viral clearance only if the cccDNA is disrupted or silenced while replication of new HBV is stopped. HBV rebounds after cessation of treatment with currently approved nucleoside analog inhibitors. To address this issue, novel antiviral agents are now being investigated including entry inhibitors, hepatitis B surface antigen (HBsAg) inhibitors and capsid assembly modulators (CAM) (5).

HBV capsid assembly plays an essential role in many steps of the viral replication cycle (6). Notably, HBV capsid is responsible for trafficking relaxed circular DNA (rcDNA) to the nucleus thereby establishing and maintaining cccDNA levels as a "refill" mechanism. Further, the HBV capsid protein is found in the nucleus of hepatocytes and interacts with host factors responsible for transcriptional regulation (7). Therefore, it is hypothesized that targeting disruption of the nucleocapsid could impact cccDNA stability and potentially lead to eradication of HBV (8). Based on the promise of sustained antiviral activity, several CAM have been studied such as GLS-4 (**1**) (phase II) (9), RG-7907 (Roche, phase I), AT-130 (**2**) (10), DVR-23 (11), NVR 3-778 (**3**) (12) (Novira/JnJ, phase IIa), AB-423 (13) and AB-506 (14) (Arbutus), JNJ-379 (Phase IIa) (15) and ABI H0731 (16) (Assembly Bioscience, Phase 1a) (**SI Appendix, Fig. S1**). Structurally these compounds are heteroaryldihydro-pyrimidines (HAPs), phenylpropenamides (PP) or sulfamoylbenzamides (SBA). Here we report the discovery and the preclinical characterization of GLP-26, a novel CAM with a unique glyoxamidopyrrolo backbone, obtained through chemical optimization of early SBA derivatives identified by our team (17).

GLP-26 (**Fig. 1**) is an HBV capsid assembly modulator displaying substantial effects at low nanomolar ranges on both HBV DNA replication and HBV e antigen (HBeAg) secretion, with greater than 1 log reduction of cccDNA amplification along with promising pre-clinical profile. Most interestingly, sustained decreases in HBeAg and HBV surface antigen (HBsAg) levels were observed in an HBV-infected humanized mouse model treated with GLP-26 in combination with entecavir up to 3 months after drug cessation.

Results

GLP-26 is a non-toxic inhibitor of HBV DNA, HBeAg and cccDNA production *in vitro*.

The *in vitro* anti-HBV activity of GLP-26 was determined by measuring secreted HBV DNA from HepAD38 cells and from infected primary human hepatocytes (PHH). GLP-26 displayed potent antiviral activity, with EC_{50} of 0.003 μM and 0.04 μM in HepAD38 cells (**Table 1**) and PHH (**Table 2**), respectively. GLP-26 did not show toxicity up to 100 μM in human hepatoma cell lines (HepG2) nor in a panel of other relevant cell types (**SI Appendix, Table S1**) yielding a wide selectivity index (SI, HepG2 cells > 33,333). It is noteworthy that GLP-26 was 25-120x more potent in these assays than GLS4, a CAM currently evaluated in the clinic. In addition, GLP-26 did not show signs of mitochondrial toxicity at concentrations up to 50 μM and no increase in lactic acid production (% of lactic acid/ % of nuclear DNA) was observed at concentrations up to 25 μM, which is well above the $EC_{50/90}$ antiviral values (**SI Appendix, Table S2**). As a correlate to cccDNA levels, GLP-26 was evaluated for inhibition of HBeAg production in HepAD38 cells (18). GLP-26 effectively inhibited HBeAg secretion with an EC_{50} = 0.003 μM, which was over 50 times more potent than GLS4 (EC_{50} = 0.16 μM, *data not shown*). As expected, the nucleoside analog 3TC had minimal effect on inhibition of HBeAg secretion (**Fig. 2A**). The same system was used to investigate the effects of agents on cccDNA using RT-qPCR. Both GLP-26 and GLS-4 equally exhibited potent inhibition of HBV cccDNA amplification, with > 1 log reduction relative to untreated mock control (**Fig. 2B**).

GLP-26 stabilizes HBV capsid particles and induces their accumulation in the cytoplasm.

Direct binding of GLP-26 to HBV capsid protein was evaluated using a fluorescent thermal shift assay by measuring changes in the thermal stability of capsids upon complexation with GLP-26 (19). The HBV capsid

protein fragment 1-149aa (Cp149) was expressed and isolated as dimers as previously described, and capsid particles were formed from Cp149 dimers by decreasing pH and increasing salt concentration. GLP-26 reproducibly increased the melting temperature of HBV Cp149 capsids (T_m = 87 ± 0.3^{o}C) to a greater extent than GLS4 (T_m = 85 ± 0.3^{o}C) (**Fig. 3A**). Fitting the titration of GLP-26 to HBV Cp149 capsids provides a K_d = 0.7 ± 1.5 μM which was ~60x fold lower than GLS4 (K_d = 41 ± 13 μM) indicating that GLP-26 binds to and stabilizes HBV capsids.

The effect of GLP-26 on cellular localization of capsids was determined by confocal microscopy in HepAD38 cells (**SI Appendix, Fig. S3)**. In the absence of drug (**Fig. 3B**), 50% of the cells contained HBV core proteins corresponding to HBV capsids in both the nucleus and the cytoplasm. In contrast, treatment with GLP-26 for 24 h emptied the nucleus and led to an accumulation of capsid particles exclusively in the cytoplasm (**Fig. 3C**) while with GLS4, capsids formed large aggregates spread in the cell (**Fig. 3D**) as previously reported for this type of HAP derivatives. (20, 21, 22, 23)

GLP-26 induces the formation of firm HBV capsid particles.

The effects of GLP-26 on capsid assembly were observed using negative-stain electron microscopy (TEM). To determine the effects on the assembly process, Cp149 dimers were first incubated with drug followed by addition of salt to initiate assembly. In the absence of drug, HBV capsids formed regular icosahedrons with a diameter of approximately 40 nm (**Fig. 4A-B**). Addition of GLP-26 to Cp149 dimers followed by assembly generated clusters of small and misshapen particles in contrast to the large, aberrant capsid morphologies observed induced by GLS4 (**SI Appendix, Fig. S4**). To determine the effects post-assembly, images of pre-formed HBV capsid particles treated with compounds were collected. Addition of GLS4 to pre-formed capsids resulted in larger, broken assemblies, similar in appearance to cracked egg shells (**SI Appendix, Fig. S4**). Unlike GLS4, fewer particles were observed upon addition of GLP-26, and those that remained exhibited smaller and firmer morphologies like “hard boiled eggs” (**Fig. 4E-F**).

GLP-26 demonstrated synergistic antiviral activity with nucleoside analogs *in vitro*.

Anticipating that HBV CAMs such as GLP-26 will be administered in combination with existing direct acting agents, we evaluated its interaction with entecavir (ETV), a potent nucleoside analog inhibitor of HBV replication. For the median-effect analysis, the drugs were combined at a 5:1 ratio (GLP-26 + ETV) based on their EC_{50} values. These two agents resulted in a combination index (CI) of 0.6 (**SI Appendix, Table S3**) indicating that GLP-26 interacted synergistically with ETV in the HepAD38 system.

GLP-26 has a favorable *in vitro* and *in vivo* pharmacokinetic profile.

In preparation for *in vivo* applications, the stability of GLP-26 was evaluated. GLP-26 demonstrated favorable stability profiles in plasma with half-lives > 24 h in human, mouse, and dog and a $t_{½}$ of ~ 8.5 h in rat plasmas (**SI Appendix, Table S4**). Liver microsome stability was also satisfactory with $t_{½}$ of 71 min and 7.6 h in mouse and human respectively (**SI Appendix, Table S6**).

The pharmacokinetic characteristics of GLP-26 were evaluated in CD-1 mice where it displayed favorable oral bioavailability (**SI Appendix, Figure S5**) with $AUC_{0\text{-}7h}^{obs}$ of 1,587 and 1,306 hr.ng/mL by oral (PO) and intravenous (IV) routes respectively. The t½ was much longer from PO administration (> 6 h) compared to that from IV (1.5h), providing prolonged concentrations high above the *in vitro* EC_{50}. Due to the favorable oral absorption profile and long half-life, we decided to deliver GLP-26 *in vivo* using oral dosing.

GLP-26 decreases HBV DNA, HBsAg and HBeAg levels in HBV-infected humanized mice.

To evaluate GLP-26 activity *in vivo*, HBV-infected BRGS-uPA mice with chimeric humanized livers (HUHEP mice) (24, 25) were treated with either GLP-26 alone (60 mg/kg/day) or in combination with ETV (0.3 mg/kg/day) by oral administration (**Fig. 5A-D**). At the start of treatment all mice had serum hAlb levels above 100 µg/ml and serum HBV DNA levels above 10^6 copies/ml. Over a period of 10 weeks, the untreated cohort increased HBV DNA (>1 log10) and HBsAg (0.5-2 log10) with no significant change in HBeAg expression. Treatment with GLP-26 alone led to decreases in viral loads (1-3 log10), HBsAg (0.3-2 log10)

and HBeAg (0.3-1 log10). In comparison, mice treated with ETV alone had a 2.7-3.3 log10 decrease in HBV DNA (one mouse had levels below limits of detection); however, the ETV-treated group showed minimal decreases in HBsAg and HBeAg (0.7 log10 and 0.2 log10, respectively).

GLP-26 and ETV act synergistically to reduce viral DNA and antigens with long-term sustained activity post-treatment in HBV-infected humanized mice.

Based on our *in vitro* results showing a synergistic effect between capsid assembly modulator GLP-26 and nucleoside analog ETV, a similar combination was evaluated *in vivo*. HBV-infected mice were treated concomitantly with both agents for 10 weeks. In the six mice treated with combination ETV (0.3 mg/kg/day) + GLP-26 (60 mg/kg/day), viral loads strongly decreased with a mean -4 log10 HBV DNA and half the mice had undetectable viremia at the end of treatment (**Fig. 5A**). Furthermore, all the mice had significantly decreased viral antigen loads – mean -1.8 log10 HBsAg and -1 log10 HBeAg (**Fig. 5B-C**).

As half the mice in the ETV + GLP-26 group had viral loads below the limit of detection after 10 weeks, viral kinetics were monitored for 11-12 weeks post-treatment cessation. During the rebound phase, viral loads returned rapidly in HBV-infected HUHEP mice that had received ETV alone, consistent with previous results (26). However, in the ETV+GLP-26 combination treatment group, of the three mice that had undetectable viremia, two remained aviremic for several weeks. HBV DNA was undetectable in one mouse for 5 weeks and the other for 11 weeks off treatment (**Fig. 5A**). Interestingly, even if HBeAg levels remained stable or slightly increased in most mice during the rebound phase, reduction of HBeAg up to -2 log10 was observed in two mice (**Fig. 5C**). HBsAg levels decreased substantially even after treatment cessation with the exception of two mice. One mouse showed undetectable levels of HBsAg (lower limit of detection = 0.1 IU/ml) despite being weakly viremic (**Fig. 5B**).

Discussion

159 Current treatments for chronic HBV are limited to nucleoside polymerase inhibitors and/or PEG-interferon.
160 These strategies rarely achieve functional cure and development of novel therapeutic agents interfering with
161 other essential steps of the viral replication cycle are needed. GLP-26 is a novel nontoxic CAM that displays
162 low nanomolar activity against HBV in both HepAD38 and PHH cells. GLP-26 is highly specific for HBV
163 and did not show activity against a panel of viruses including Dengue virus, West Nile virus, Chikungunya
164 virus, Zika virus and HIV-1 up to 30 µM (**SI Appendix, Table S6**). Unlike heteroaryldihydropyrimidine
165 derivatives (HAP) such as GLS4, GLP-26 binds to the capsid and induces formation of tight, intact particles.
166 These biochemical outcomes are similar to those observed for the alternate class of CAMs that includes the
167 propenamides (AT-130) and sulfamoylbenzamides (SBA, such as AB-423 or NVR-3-778) derivatives.
168 GLP-26 decreases cccDNA *in vitro* and decreases HBeAg (a biomarker of cccDNA) levels *in vitro* and *in*
169 *vivo.* HBV maintains cccDNA levels by recycling mature relaxed circular (rc) DNA to the nucleus (27). This
170 process relies on the proper biophysical properties of HBV capsid protein for rcDNA formation and nuclear
171 transport. Since GLP-26 affects capsid assembly and possibly transport into the nucleus, the agent likely
172 disrupts cccDNA maintenance from this cycle leading to an overall reduction in cccDNA levels.
173 GLP-26 in combination with ETV potently decreased HBsAg and HBeAg levels in a humanized mouse model
174 of infection both during and more importantly after treatment. It is worth noting that previous studies have
175 shown decreased HBV viral antigens during combination treatments (28), yet continued antiviral effects on
176 these markers after treatment have not been yet reported for other CAMs from the same class (AB-423 and
177 JNJ-632 respectively) (13, 29). The mechanisms resulting in sustained response could arise from the very
178 potent antiviral activity of GLP-26 (10-100 times more potent than AB-423 and JNJ-632) combined with a
179 prolonged exposure from oral administration leading to sustained efficacious levels of GLP-26. Since HBsAg
180 seroconversion is more likely with low levels of HBsAg (30), these observations suggest there is potential for
181 seroconversion when these biomarkers are decreased with GLP-26 treatment. In addition, the model used in

this study did not reconstitute the mice with humanized immune systems, and we anticipate improved activity and seroconversion in immunocompetent animal models or humans upon treatment with GLP-26. Overall, GLP-26 displayed favorable metabolic stability with high oral bioavailability and no adverse effects were observed after oral administration for up to 10 weeks, highlighting the relative safety of this compound. Optimization of the treatment period, oral dosing and drug combinations (ETV, pegIFN, etc.) will be essential to deliver a more pronounced and lasting antiviral effect in animal models and eventually in humans.

Conclusion: We identified GLP-26 as a highly potent and promising HBV CAM. Direct effects of GLP-26 on HBV capsid assembly was established using electron microscopy, confocal microscopy and thermal shift assays. GLP-26 inhibited HBV DNA, HBeAg and cccDNA amplification and did not display any toxicity *in vitro*. Oral bioavailability in mice and stability in both plasma and liver microsomes strengthen an already excellent preclinical profile. Combination treatment of GLP-26 with ETV in a humanized mouse model of HBV infection delivered sustained antiviral response up to 12 weeks after treatment cessation offering the hope that similar effects can be reached in humans with this novel CAM.

Materials and Methods

Synthesis of compounds. Synthesis and characterization of GLP-26 is detailed in Supplementary Information (SI) Section. GLS-4 was prepared according to the chemistry and methods previously described (31). Both compounds had a purity > 95% as determined by proton ^{13}NMR and HPLC analysis. Entecavir (ETV), lamivudine (3TC), tenofovir disoproxil fumarate (TDF) were purchased from commercial vendors and confirmed > 95% purity using standard analytical methods such as mass spectrometry and NMR.

Cytotoxicity assays. *In vitro* cytotoxicity was determined using the CellTiter 96 non-radioactive cell proliferation colorimetric assay (MTT assay, Promega) in primary human peripheral blood mononuclear cells

(PBMC), human T lymphoblast (CEM) and human hepatocellular carcinoma (HepG2) cell lines. Toxicity levels were measured as the concentration of test compound that inhibited cell proliferation by 50% (CC_{50}).

HBV Assay in HepAD38. The HBV assay was performed in HepAD38 cells as previously described (32). Briefly, HepAD38 cells were seeded onto 96-well plates and incubated for two days at 37°C in a humidified 5% CO_2 atmosphere. On day two, medium with tetracycline (Tet) was removed and cells were washed with 1X PBS. Antiviral drugs were prepared in medium without Tet and added in duplicate at various concentrations. After a total of seven days incubation, total DNA was extracted using DNeasy 96 Tissue kit (Qiagen), and HBV DNA was amplified by real-time PCR (18). Antiviral activity was measured by determining the average threshold cycle for the HBV DNA amplification with the compounds (alone or in combination), which was subtracted from the average cycle of the untreated-tetracycline control (ΔCT). Drugs were first tested individually for effective concentration, which inhibited 50% and 90% of HBV DNA replication (EC_{50} and EC_{90}) using CalcuSyn software program (Biosoft, Ferguson, MO, USA).

Evaluation of HBeAg secretion. The effect of GLP-26 on the levels of cccDNA amplification was assessed using the HepAD38 cells to measure HBeAg as a cccDNA-dependent marker (33). In this system, HBV replication is controlled with tetracycline: its presence in the medium blocks pre-genomic (pg) RNA synthesis, and in its absence, synthesis of pgRNA and HBV DNA replication occur. In addition, when cells are re-treated with Tet, new cccDNA formation is restored and HBe Ag production can be measured as a reporter for levels of intracellular cccDNA. HepAD38 cells were incubated with or without test compounds for seven days in medium without Tet, and another seven days in medium with Tet when cccDNA formation and virus production relies exclusively on restored cccDNA and not on the transgene. Supernatants were harvested at day-14, clarified by centrifugation at 2,550 x g for 5 min, and stored at -70°C until use. Levels of HBeAg secreted in the culture medium were measured by using HBeAg ELISA kit (BioChain Institute Inc.

Hayward, CA) according to the manufacturer's protocol. The concentration of compound that reduced levels of secreted HBeAg by 50% (EC_{50}) was determined by linear regression.

Evaluation of Intracellular HBV DNA and cccDNA Levels. DNA was extracted from HepAD38 cells for cccDNA detection. On day 14 of the experiments, DNA was purified from cells using a commercially available kit (Plasmid Miniprep Kit, Qiagen) or a modified Hirt extraction (34). All samples were treated with plasmid-safe adenosine triphosphate (ATP)-dependent deoxyribonuclease (PSAD) (Epicentre, Lucigen Corporation, Middleton, WI) at 37^{o}C for 18 h, followed by incubation at 70^{o}C for 30 min to inactivate PSAD. For HBV cccDNA amplification, we used TaqMan primers as previously shown (35) to specifically amplify cccDNA (forward primer: 5' ACTCTTGGACTCBCAGCAATG3', reverse primer: 5'-CTTTATACGGGTCAATGTCCA-3', and probe: 5'-FAM-CTTTTTCACCTCTGCCTAATCATCTCWTGTTCA-TAMRA-3') using the LightCycler 480 instrument (Roche).

Anti-HBV Evaluation in Primary Human Hepatocytes (PHH). PHH were seeded on collagen-coated 48-well plates at 1.4x10^{5} cells/well in InVitroGro CP (BioIVT) medium for three hours, and then replenished with maintenance HI medium - InVitroGro HI plus Torpedo antibiotic mix (BioIVT). After 24 h, cells were incubated with HBV inoculum at multiplicity of infection (MOI) of 1,000 genome equivalent per cell in maintenance HI medium containing 4% PEG-8000. The HBV inoculum was removed 24 h post infection, and the cultures were maintained in HI medium for four days. Infected PHH cells were then incubated with the indicated concentrations of test compounds for seven days, when the medium with or without compound was replenished. After a total of 10 days, supernatants were harvested and HBV DNA production was quantified by qRT-PCR using the following HBV specific primers: HBV-AD38-qF1 (5'-CCGTCT GTG CCT TCT CAT CTG-3'), HBV-AD38-qR1 (5'- AGT CCA AGA GTY CTC TTATRY AAG ACC TT-3'), and HBV-AD38-qP1 (5'-FAM-CCG TGT GCA /ZEN/CTT CGCTTC ACC TCT GC-3'BHQ1).

Electron Microscopy. Samples of HBV Cp149 dimers and capsids were prepared as previously described (17). Samples were fixed onto a charged carbon grid and stained by uranyl acetate contrast agent for 15 min. EM images were collected using a JEOL JEM-1400 electron microscope operating at 120 kV at 25,000 - 35,000 x magnification (Emory University Robert P. Apkarian electron microscopy core facility).

Thermal Shift Fluorescence Assay. Samples were prepared containing 2 µM HBV Cp149 capsids and varying concentrations of compounds (1-80 µM) with < 1% DMSO to a final volume of 40 µL. Sypro orange was added to each well at 2 µL of 1:50 dilution. Each measurement was made in triplicate across two samples. Sypro orange fluorescence was monitored continuously as temperature scanned from 45-95^{o}C at a rate of 1^{o}C/min on a Light Cycler 480 (Roche).

Confocal microscopy. Experiments were performed on HepAD38 cells. Cells were maintained in DMEM supplemented with 10% fetal bovine serum (Gibco, France) and 1% antibiotics (penicillin/streptomycin: Gibco, France) at 37^{o}C in 5% CO_2. HepAD38 cells were seeded for 6 hours, washed and incubated in DMEM. Next, 1% v/v DMSO or 100 µM of GLP-26 (in 1% v/v DMSO) were added to this medium. After 24 h of treatment, the medium was refreshed and cells were incubated for additional 24 h. HepAD38 cells were fixed with 4% paraformaldehyde/PBS, permeabilized with 0.2% triton/PBS and blocked for 45 min with 0.4% of BSA. Cells were then incubated with a human anti-HBc antibody (36) and after successive washing in PBS, with Alexa fluor 488 goat anti-human (ThermoFisher scientific). The last wash contained DAPI and cells were kept in PBS at 4^{o}C until observation. Fluorescence confocal images were taken using a confocal microscope LEICA SP8 gSTED equipped with 63x PL APO 1.40 CS2 Oil, a laser diode at 405 nm for DAPI and an argon laser at 488 nm for Alexa 488.

Drug Combination Study. Drug interactions were analyzed using CalcuSyn (Biosoft, Ferguson, MO, USA) computer software For the median-effect analysis, the drugs were combined at a 5:1 ratio (GLP-26 + entecavir

- ETV) based on their EC_{50} values. Five to six concentrations of each single drug, or in combination, were performed in at least two independent experiments (37).

Stability in Mouse, Rat, Dog and Human Plasma. One mL of mouse, rat, dog or human plasma containing 5 mM $MgCl_2$ were used for the stability assay. Propantheline bromide at 10 µM was used as a positive control. The reaction was started by adding 10 µL of 1 mM stock solution of GLP-26 to give a final concentration of 10 µM and incubated at 37°C. At selected times (0, 0.25, 0.5, 1, 2, 4, 6 and 24 h), 100 µL aliquots were taken and the reaction was stopped by mixing with 400 µL of ice-cold acetonitrile. The samples were centrifuged and 100 µL of the supernatant was mixed with 100 µL of LC-MS mobile phase then subjected to LC-MS/MS analysis.

Stability in Mouse and Human Liver Microsomes. The reaction mixture was prepared in a total volume of 1.5 mL containing 5 mM of $MgCl_2$, 100 mM of potassium phosphate buffer (pH 7.4), 1 mg/mL mouse or human liver microsome and 1 µM compound. The reaction was initiated by adding 1 mM NADPH to the mixture and incubated at 37°C. At selected times (0, 5, 15, 30, 45, 60 and 90 min), 200 µL aliquots were taken and the reaction stopped by mixing with 200 µL of 70% ice-cold methanol. The samples were centrifuged and supernatant were subjected to LC-MS/MS analysis. Propranolol at 10 µM was used as a positive control.

Pharmacokinetic Studies: GLP-26 (3 mg/mL) in PBS containing 20% DMSO and 20% PEG-400, was given by intravenous (IV) injection (15 mg/kg) and orally (PO) 30 mg/kg to female CD-1 mice. At the given time points (0.5 h, 2 h, 4 h, and 7 h), blood samples were collected using heparinized capillaries. Samples were centrifuged at 15,000 g for 10 min. Subsequently, blood plasma was collected and frozen at -80°C until analysis using LC-MS/MS (ACQUITY UPLC BEH C18 Column, 130Å, 1.7 µm, 3 mm X 30 mm and Turbo-IonsprayTM Interface in the negative ion-mode on AB Sciex 5500Qtrap). IACUC approval was obtained prior to initiation of these mouse studies.

Generation of HUHEP Mice, HBV Infection and Treatment. BALB/c Rag2$^{-/-}$IL-2Rγc$^{-/-}$NOD.*sirpa* uPA$^{tg/tg}$ (BRGS-uPA) mice were intrasplenically injected with 7 x 10^5 freshly thawed human hepatocytes (BD Biosciences, Corning) to generate HUHEP mice as previously described (25). Liver chimerism of HUHEP mice was evaluated with a species-specific human albumin (hAlb) ELISA (Bethyl Laboratories) on plasma samples as previously described (25). HUHEP mice with ≥100 µg/ml hAlb were intraperitoneally infected with 1x10^7 HBV genome equivalents as previously described (24). HBV-infected mice with >10^6 HBV DNA copies/ml were treated *per os* with either ETV 0.3 mg/kg/day (Baraclude, BMS), or GLP-26 60 mg/kg/day (dissolved in PEG400, Sigma), or the combination of ETV+GLP-26 at the same doses, delivered in MediDrop Sucralose (Clear H_2O) continuously for 10 weeks. For the rebound phase, mice were returned to regular drinking water. Animals were housed in isolators under pathogen-free conditions with humane care. Experiments were approved by an institutional ethical committee at the Institut Pasteur (Paris, France) and validated by the French Ministry of Education and Research (MENESR # 02162.02).

Virological Measurements in HUHEP Mice. HBV DNA was extracted from plasma and quantified by qPCR as previously described (24). HBeAg was quantified with an ELISA chemiluminescent immunoassay kit (Autobio, China), and HBsAg was quantified with the MONOLISA HBsAg Ultra kit (Bio-Rad) following manufacturer's protocols.

ACKNOWLEDGMENT: This work was supported in part by NIH Grant 1-R01-AI-132833 (RFS), and 5P30-AI-50409 (CFAR) (RFS), by Agence Nationale de Recherches sur le Sida et les Hépatites Virales (ANRS) Grants #2016-16180 and #2016-16365, European Commission Seventh Framework Programme PATHCo (HEALTH-F3-2012-305578), Institut Pasteur, and Institut national de la santé et de la recherche médicale (HSM); by ANRS and Institut national de la santé et de la recherche médicale (INSERM) (HDR). We gratefully acknowledge the Center for Translational Science and the Animalerie Centrale of the Institut

316 Pasteur for productive collaboration. We also thank Pierre-Ivan Raynal and Julien Burlaud-Gaillard from
317 Electron Microscopy (EM) Facility (IBiSA) of the Tours University (http://microscopies.med.univ-tours.fr)
318 for technical support. We gratefully acknowledge Elizabeth Wright, Ph.D. (University of Wisconsin,
319 Madison) and Hong Yi (Emory University Robert P. Apkarian electronmicroscopy core) for their advice and
320 assistance with the EM studies.

321

322 **REFERENCES**

323 1. From WHO website (July 2018): http://www.who.int/news-room/fact-sheets/detail/hepatitis-b

324 2. a) Locarnini S, Zoulim F. 2010. Molecular genetics of HBV infection. Antivir Ther 15, Suppl 3:3-14; b)
325 Schadler S; Hildt E. 2009. HBV life cycle: entry and morphogenesis. Viruses 1:185-209.

326 3. Block TM, Guo H, Guo JT. 2007. Molecular virology of hepatitis B virus for clinicians. Clin Liver Dis
327 11:685-706.

328 4. Cai D, Mills C, Yu W, Yan R, Aldrich CE, Saputelli JR, Mason WS, Xu X, Guo JT, Block TM, Cuconati
329 A, Guo H. 2012. Identification of disubstituted sulfonamide compounds as specific inhibitors of hepatitis B
330 virus covalently closed circular DNA formation. Antimicrob Agents Chemother 56:4277-4288.

331 5. Kim WR. 2018. Emerging therapies toward a functional cure for hepatitis B virus infection. Gastroenterol
332 Hepatol (N Y) 14: 439-442.

333 6. Cole AG. 2016. Modulators of HBV capsid assembly as an approach to treating hepatitis B virus infection.
334 Curr Opin Pharmacol 131-137.

335 7. Diab A, Foca A, Zoulim F, Durantel D, Andrisani O. 2018. The diverse functions of the hepatitis B
336 core/capsid protein (HBc) in the viral life cycle: implications for the development of HBc-targeting antivirals.
337 Antiviral Res 149:211-220.

338 8. Boucle S, Bassit L, Ehteshami M, Schinazi RF. 2016. Toward elimination of hepatitis B virus using novel
339 drugs, approaches, and combined modalities. Clin Liver Dis 20:737-749.
340 9. Wu G, Liu B, Zhang Y, Li J, Arzumanyan A, Clayton MM, Schinazi RF, Wang Z, Goldmann S, Ren Q,
341 Zhang F, Feitelson MA. 2013. Preclinical characterization of GLS4, an inhibitor of hepatitis B virus core
342 particle assembly. Antimicrob Agents Chemother 57:5344-54.
343 10. Katen SP, Chirapu SR, Finn MG, Zlotnick A. 2010. Trapping of hepatitis B virus capsid assembly
344 intermediates by phenylpropenamide assembly accelerators. ACS Chem Biol 5:1125-1136.
345 11. Campagna MR, Liu F, Mao R, Mills C, Cai D, Guo F, Zhao X, Ye H, Cuconati A, Guo H, Chang J, Xu X,
346 Block TM, Guo JT. 2013. Sulfamoylbenzamide derivatives inhibit the assembly of hepatitis B virus
347 nucleocapsids. J Virol 87:6931-6942.
348 12. a) Gane EJ, Schwabe C, Walker K, Flores L, Hartman GD, Klumpp K, Liaw S, Brown NA. 2014. Phase
349 1a safety and pharmacokinetics of NVR 3-778, a potential first-in-class HBV core inhibitor. Hepatology
350 60:LB19. b) Lam AM, Espiritu C, Vogel R, Ren S, Lau V, Kelly M, Kuduk SD, Hartman GD, Flores OA,
351 Klumpp K. 2018. Preclinical characterization of NVR 3-778, a first-in-class capsid assembly modulator
352 against hepatitis B virus. Antimicrob Agents Chemother 63: e01734-18.
353 13. Mani N, Cole AG, Phelps JR, Ardzinski A, Cobarrubias KD, Cuconati A, Dorsey BD, Evangelista E, Fan
354 K, Guo F, Guo H, Guo JT, Harasym TO, Kadhim S, Kultgen SG, Lee ACH, Li AHL, Long Q, Majeski SA,
355 Mao R, McClintock KD, Reid SP, Rijnbrand R, Snead NM, Micolochick Steuer HM, Stever K, Tang S, Wang
356 X, Zhao Q, Sofia MJ. 2018. Preclinical profile of AB-423, an inhibitor of hepatitis B virus pregenomic RNA
357 encapsidation Antimicrob Agents Chemother 62:e00082-18.
358 14. Mani N, Li AHL, Ardzinski A, Bailey L, Phelps JR, Burns R, Chiu T, Cole AG, Cuconati, A, Dorsey BD,
359 Evangelista E, Gotchev D, Harasym TO, Jarosz A, Kadhim S., Kondratowicz A., Kultgen SG, Kwak K, Lee
360 ACH, Majeski S, Mcclintock K, Pan J, Pasetka C, Rijnbrand R, Shapiro A, Steuer HM, Stever K, Tang S,

Teng X, Wong M, Sofia MJ. 2018 Preclinical antiviral drug combination studies utilizing novel orally bioavailable investigational agents for chronic hepatitis B infection: AB-506, a next generation HBV capsid inhibitor, and AB-452, an HBV RNA destabilizer. J Hepatol 68:S17.

15. https://clinicaltrials.gov/ct2/show/NCT03361956

16. Yuen MF, Agarwal K, Gane G, Schwabe C, Cheng W, Sievert W, Kim DJ, Ahn SH, Lim Y-S, Visvanathan K, Ruby E, Liaw S, Colonno R, Lopatin U. 2018. Interim safety, tolerability pharmacokinetics, and antiviral activity of ABI-H0731, a novel core protein allosteric modulator, in healthy volunteers, and non-cirrhotic viremic subjects with chronic hepatitis B. J Hepatol 68:S111.

17. Sari O, Boucle S, Cox BD, Ozturk T, Russell O, Bassit L, Amblard F, Schinazi RF. 2017. Synthesis of sulfamoylbenzamide derivatives as HBV capsid assembly effector. Eur J Med Chem 138:407-421.

18. Pas SD, Fries E, De Man RA, Osterhaus AD, Niesters HG. 2000. Development of a quantitative real-time detection assay for hepatitis B virus DNA and comparison with two commercial assays. J Clin Microbiol 38:2897-2901.

19. a) Lo MC, Aulabaugh A, Jin G, Cowling R, Bard J, Malamas M, Ellestad G. 2004. Evaluation of fluorescence-based thermal shift assays for hit identification in drug discovery. Anal Biochem 332:153-159. b) Tang J, Huber AD, Pineda DL, Boschert KN, Wolf JJ, Kankanala J, Xie J, Sarafianos SG, Wang, Z. 2019. 5-Aminothiophene-2, 4-dicarboxamide analogues as hepatitis B virus capsid assembly effectors. Eur. J. Med. Chem. 164:179-192.

20. Lahlali T, Berke JM, Vergauwen K, Foca A, Vandyck K, Pauwels F, Zoulim F, Durantel D. 2018. Novel potent capsid assembly modulators regulate multiple steps of the Hepatitis B virus life-cycle. Antimicrob Agents Chemother.

21. Huber AD, Wolf JJ, Liu D, Gres AT, Tang J, Boschert KN, Puray-Chavez MN, Pineda DL, Laughlin TG, Coonrod EM, Yang Q, Ji J, Kirby KA, Wang Z, Sarafianos SG. 2018. The heteroaryldihydropyrimidine Bay 38-7690 induces hepatitis B virus core protein aggregates associated with promyelocytic leukemia nuclear bodies in infected cells. mSphere 3, e00131-18.

22. Corcuera A, Stolle K, Hillmer S, Seitz S, Lee J-Y, Bartenschlager R, Birkmann A, Urban A. 2018. Novel non-heteroarylpyrimidine (HAP) capsid assembly modifiers have a different mode of action from HAPs in vitro. Antivir. Res. 158:135-42.

23. Rat V, Seigneuret F, Burlaud-Gaillard J, Lemoine R, Hourioux C, Zoulim F, Testoni B, Meunier JC, Tauber C, Roingeard P, de Rocquigny H. 2019. BAY 41-4109-mediated aggregation of assembled and misassembled HBV capsids in cells revealed by electron microscopy. Antiv. Res. 169:104557.

24. Dusséaux M, Masse-Ranson G, Darche S, Ahodantin J, Li Y, Fiquet O, Beaumont E, Moreau P, Rivière L, Neuveut C, Soussan P, Roingeard P, Kremsdorf D, Di Santo JP, Strick-Marchand H. 2017. Viral load affects the immune response to HBV in mice with humanized immune system and liver. Gastroenterology 153:1647-1661.

25. Strick-Marchand H, Dusséaux M, Darche S, Huntington ND, Legrand N, Masse-Ranson G, Corcuff E, Ahodantin J, Weijer K, Spits H, Kremsdorf D, Di Santo JP. 2015. A novel mouse model for stable engraftment of a human immune system and human hepatocytes PLoS One 10:e0119820

26. Mueller H, Wildum S, Luangsay S, Walther J, Lopez A, Tropberger P, Ottaviani G, Lu W, Parrott NJ, Zhang JD, Schmucki R, Racek T, Hoflack JC, Kueng E, Point F, Zhou X, Steiner G, Lütgehetmann M, Rapp

404 G, Volz T, Dandri M, Yang S, Young JAT, Javanbakht H. 2018. A novel orally available small molecule that
405 inhibits hepatitis B virus expression. J Hepatol 68:412-420.
406 27. Zlotnick A, Venkatakrishnan B, Tan Z, Lewellyn E, Turner W, Francis S. 2015. Core protein: A
407 pleiotropic keystone in the HBV lifecycle. Antiviral Res 121: 82-93.
408 28. Klumpp K, Shimada T, Allweiss L, Volz T, Lütgehetmann M, Hartman G, Flores OA, Lam AM, Dandri
409 M. 2018. Efficacy of NVR 3-778, Alone and in combination with pegylated Interferon, vs entecavir in
410 uPA/SCID mice with humanized livers and HBV infection. Gastroenterology 154:652-662.
411 29. Vandyck K, Rombouts G, Stoops B, Tahri A, Vos A, Verschueren W, Wu Y, Yang J, Hou F, Huang B,
412 Vergauwen K, Dehertogh P, Berke JM, Raboisson P. 2018. Synthesis and evaluation of N-phenyl-3-
413 sulfamoyl-benzamide derivatives as capsid assembly modulators inhibiting hepatitis B virus (HBV). J Med
414 Chem 61:6247-6260.
415 30. Tseng TC, Liu CJ, Su TH, Wang CC, Chen CL, Chen PJ, Chen DS, Kao JH. 2011. Serum hepatitis B
416 surface antigen levels predict surface antigen loss in hepatitis B e antigen seroconverters. Gastroenterology
417 141:517–525, 525.e511–e512.
418 31. Ren Q, Liu X, Luo Z, Li J, Wang C, Goldmann S, Zhang J, Zhang Y. 2017 Discovery of hepatitis B virus
419 capsid assembly inhibitors leading to a heteroaryldihydropyrimidine based clinical candidate (GLS4). Bioorg
420 Med Chem 25:1042-1056.
421 32. Ladner SK, Otto MJ, Barker CS, Zaifert K, Wang GH, Guo JT, Seeger C, King RW. 1997. Inducible
422 expression of human hepatitis B virus (HBV) in stably transfected hepatoblastoma cells: a novel system for
423 screening potential inhibitors of HBV replication. Antimicrob Agents Chemother 41:1715-1720.
424 33. Zhou T, Guo H, Guo JT, Cuconati A, Mehta A, Block TM. 2006. Hepatitis B virus e antigen production is
425 dependent upon covalently closed circular (ccc) DNA in HepAD38 cell cultures and may serve as a cccDNA
426 surrogate in antiviral screening assays. Antiviral Res 72:116-124.

34. Guo H, Jiang D, Zhou T, Cuconati A, Block TM, Guo JT. 2007. Characterization of the intracellular deproteinized relaxed circular DNA of hepatitis B virus: an intermediate of covalently closed circular DNA formation. J Virol 81:12472-12484.

35. Chen Y, Sze J, He ML. 2004. HBV cccDNA in patients' sera as an indicator for HBV reactivation and an early signal of liver damage. World J Gastroenterol. 10(1):82-85.36. Roingeard P, Romet-Lemonne JL, Leturcq D, Goudeau A, Essex M. 1990. Hepatitis B virus core antigen (HBc Ag) accumulation in an HBV nonproducer clone of HepG2-transfected cells is associated with cytopathic effect. Virology 179:113-120.

37. Bassit L, Grier J, Bennett M, Schinazi RF. 2008. Combinations of 2'-C-methylcytidine analogues with interferon-alpha2b and triple combination with ribavirin in the hepatitis C virus replicon system. Antivir Chem Chemother 19(1):25-31.

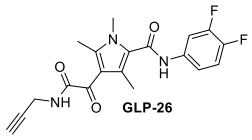

Figure 1. Structure of GLP-26.

A.

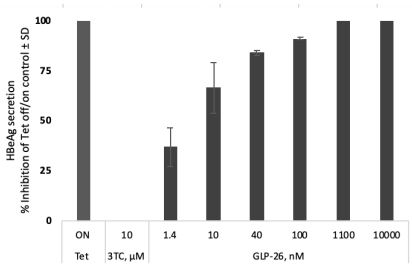

B.

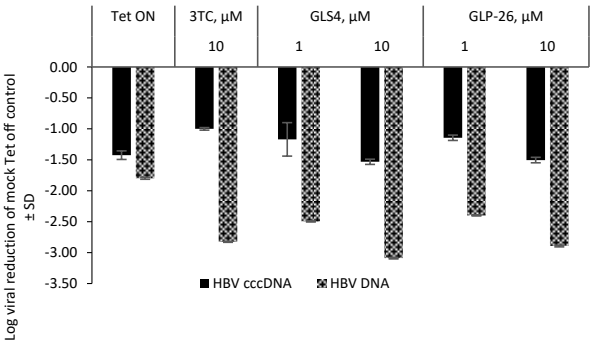

Figure 2. Decrease of cccDNA markers in HepAD38 cells by GLP-26. A) Percent inhibition of HBeAg secretion by ELISA; Cells with or without drugs were incubated in the absence of tetracycline for 7 days, followed by addition of Tet to culture of both untreated and drug-treated cells for another 7 days (7-14 days). Tet ON, cells cultured in the presence of tetracycline for 14 days. Inhibition (%) of HBeAg secretion was determined relative to untreated Tet off/on control. and B) The levels of HBV DNA and cccDNA were quantified by qPCR and log viral reduction was determined relative to untreated mock Tet off control. All values represent the average of at least two independent experiments and samples were performed in duplicate ± SD.

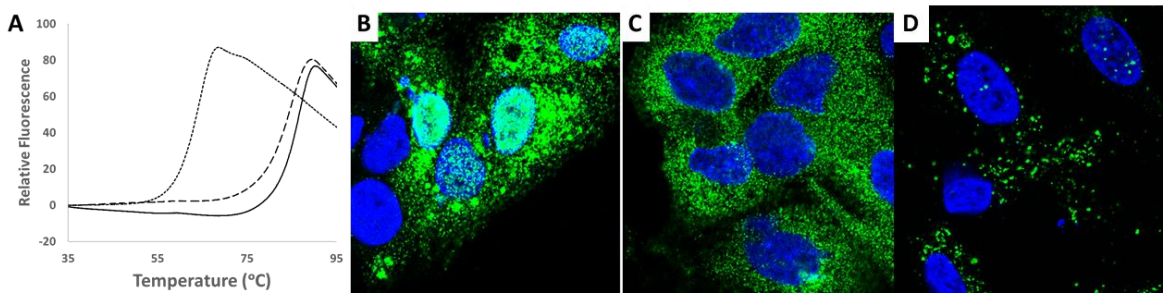

Figure 3. Effects of GLP-26 binding to HBV capsids. A) Thermal shift fluorescence assay thermograms for vehicle (dotted line), GLS4 (dashed line) and GLP-26 (solid line) treated HBV Cp149 capsids. Confocal immunofluorescence microscopy images showing HBV Core protein (in green) distribution in HepAD38 hepatocytes after 24 h for B) vehicle (DMSO) , C) GLP-26 (1 μM). D) GLS-4 (1 μM). Nuclei are DAPI stained (blue).

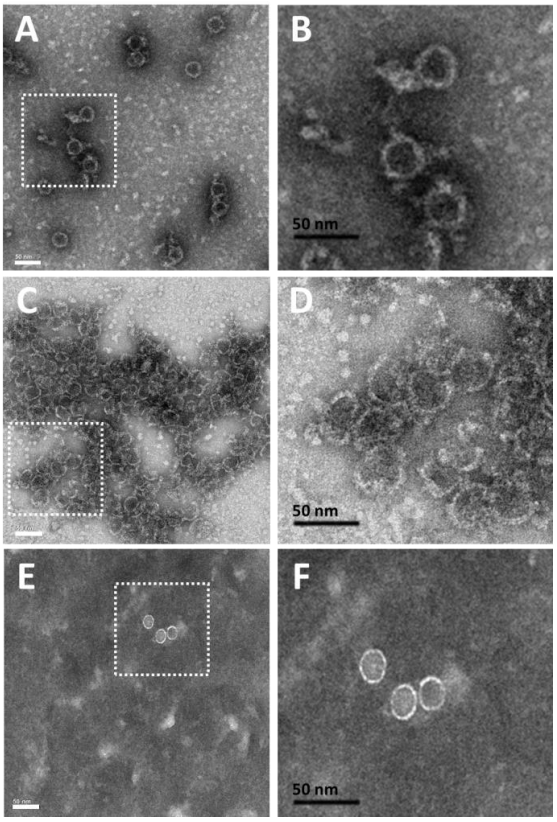

Figure 4. Effects of GLP-26 on the HBV Cp149 capsid morphology determined by negative-stain electron microscopy. A and B) HBV Cp149 capsid particles treated with vehicle and. C and D) HBV Cp149 treated with GLP-26 (25 μM) prior to assembly initiation. E and F) Pre-formed HBV-Cp149 capsid particles treated with GLP-26 (25 μM). Black bars represent 50 nm scale.

478

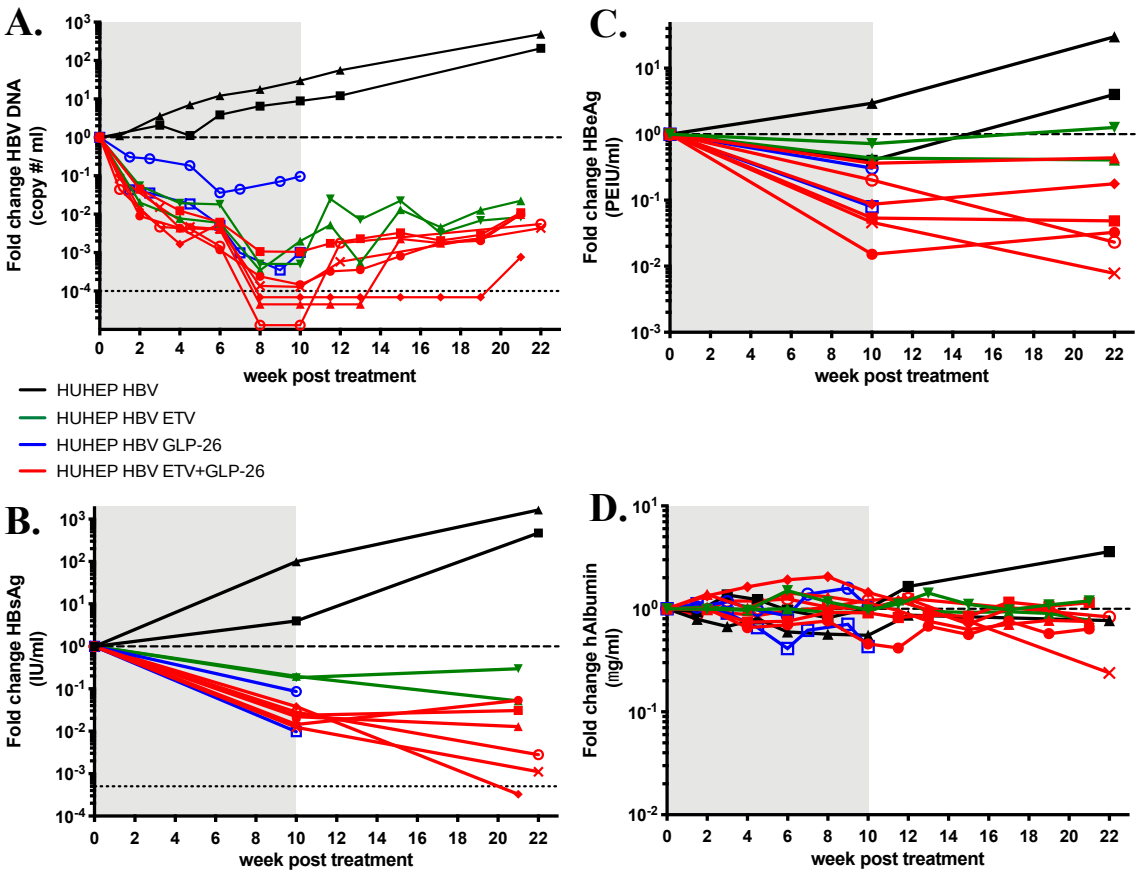

479

480

481 **Figure 5. Sustained antiviral activity of GLP-26 in HBV-infected humanized mice by oral**
482 **administration.** Effect of entecavir (ETV) 0.3 mg/kg/day, GLP-26 60 mg/kg/day or the combination of ETV
483 + GLP-26 at the same doses on A) HBV DNA, B) HBsAg, C) HBeAg, and D) human Albumin in HBV-
484 infected HUHEP mice. Treatment period is indicated in the grey shaded area followed by a rebound period,
485 the lower limit of detection is shown as a thin dotted horizontal line in A) and B). The thick dotted horizontal
486 line shows the reference point of one to evaluate fold changes. Each full line represents the longitudinal

487 results from an individual HBV-infected HUHEP mouse either untreated (black line), ETV (green line), GLP-
488 26 (blue line), or ETV+GLP-26 (red line) treated.

489

490 **Table 1.** Anti-HBV activity of GLP-26 in HepAD38 cells.

Drug[a]	Anti-HBV Activity (μM)	
	EC_{50}	EC_{90}
GLP-26	0.003 ± 0.002	0.014 ± 0.002
GLS4	0.08 ± 0.02	0.28 ± 0.06
3TC	0.41 ± 0.36	1.65 ± 0.92
ETV	0.0006 ± 0.0003	0.011 ± 0.002
TDF	0.005 ± 0.0004	0.070 ± 0.010

491 [a]3TC: Lamivudine; ETV: Entecavir. TDF: Tenofovir disoproxil fumarate

492 All values represent the average of at least two independent experiments and samples were performed in
493 duplicate ± SD.

494

495 **Table 2.** Anti-HBV activity of GLP-26 in primary human hepatocytes (PHH).

496

Drug	Anti-HBV Activity (μM)	PHH
	EC_{50}	CC_{50} (μM)
GLP-26	0.04 ± 0.01	>10
GLS4	4.34 ± 1.62	>10
TDF[a]	0.27 ± 0.23	>10

[a]TDF: Tenofovir disoproxil fumarate. All values represent the average of at least two independent experiments and samples were performed in duplicate.

497